ENCIT2024
20th Brazilian Congress of Thermal Sciences and Engineering

ABCM Associação Brasileira de Engenharia e Ciências Mecânicas

20th Brazilian Congress of Thermal Sciences and Engineering
November 10th–14th, 2024, Foz do Iguaçu - PR - Brazil

ENC-2024-0344
CHARACTERIZATION OF BOUNDARY LAYERS IN SOLAR CHIMNEYS FROM NUMERICAL SIMULATIONS WITH CFD TECHNIQUES

Daniel Croza
Pedro Galione
Facultad de Ingeniería - Universidad de la República (Julio Herrera y Reissig 565 - Montevideo, Uruguay)
dcroza@fing.edu.uy; pgalione@fing.edu.uy

Abstract. *Solar chimneys use solar energy to heat the air inside them and thus produce a density gradient there, which due to buoyancy effects results in a natural circulation of this air. They have various applications, such as thermal conditioning and passive ventilation of buildings. They can contribute to the energy efficiency of buildings, and are an interesting alternative due to their possible economic advantages, so it is important to have models that allow estimating the air flows that are achieved (and air outlet temperatures, for heating applications) based on knowing the available solar radiation. In the present work, different ways of modeling the air flow through a solar chimney are evaluated from numerical simulations with CFD techniques. Using the OpenFOAM 8 software, chimneys from an experimental work were simulated, work in which the authors built a laboratory model of a solar chimney with uniform heat flux in one of its walls, which they achieved from electrical heating. Taking only the chimney as the working domain for the simulations, different options for the boundary conditions were considered, both in the inlet and outlet sections, and in the solid walls (absorber plate and transparent cover). Some difficulties were encountered with the boundary conditions in the inlet and outlet sections, linked to the way buoyancy effects are implemented in the* `buoyantPimpleFoam` *solver in OpenFOAM version 8, which works with variable density instead of using the Bousinessq approximation. This work shows how these difficulties were overcome in this particular case, which has horizontal inlet and outlet sections. Regarding the thermal boundary conditions on the walls, it can be seen that their choice in the transparent cover strongly impacts the type of air flow obtained in the chimney and the numerical values of mass air flow rate that are reached once the simulation arrives the steady state.*

Keywords: *solar chimneys, numerical simulations, fluid mechanics, heat transfer, OpenFOAM*

1. INTRODUCTION

Figure 1 shows a diagram of a simple solar chimney consisting of a semi-transparent wall (cover plate or transparent cover), an air chamber, and an opaque wall (absorber wall or absorber plate).

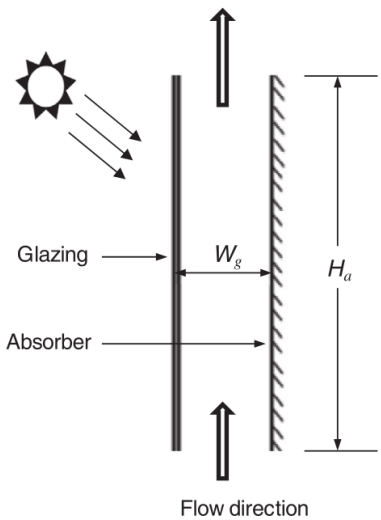

Figure 1: Solar chimney diagram. Extracted from Khanal and Lei (2014)

Its basic operation is very simple. Solar radiation passes through the transparent cover and heats the absorber wall. The absorber wall heats the air inside the chimney, and due to buoyancy effects, the hot air (lighter than the outside air)

rises through the chamber.

In building air conditioning and passive ventilation applications, solar chimneys can be used in many ways to fulfill different functions, which may vary depending on the time of year. Some of the possible operating modes of a solar chimney are shown in Fig. 2. The passive heating mode achieves warming of a room, as well as a certain degree of ventilation, in cold days. The natural ventilation mode achieves a certain degree of ventilation, and in case of an exterior temperature lower than the room temperature it also provides cooling of the room. The thermal insulation mode reduces the heat load gained by the room, when solar heat flux and exterior temperature are high.

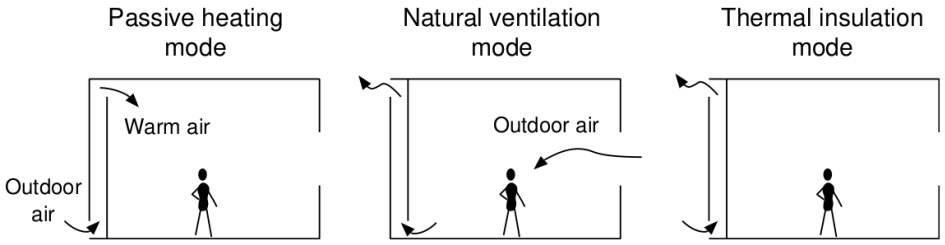

Figure 2: Operation modes of a solar chimney. Extracted from Miyazaki *et al.* (2006)

It is important to have simple models of solar chimneys that allow estimating the air flow rates achieved (and air outlet temperatures for heating applications) based on the available solar radiation. Among the simplest models of solar chimneys, the one considered in the work of Bansal *et al.* (1993) could be mentioned. Regarding the simple models that assume less simplifying hypotheses, it is worth mentioning the one developed by Kosut (2017) in his master's thesis. These simple solar chimney models can be incorporated into building energy simulation models, capable of simulating building operation over long periods of time to evaluate their energy performance, for example on annual scales. Simple models can be fed by experimental results or by more complex simulations, such as those dealt with in Computational Fluid Mechanics (CFD), to adjust parameters with the aim of obtaining greater precision in their predictions. In many works, such as the work of Zamora and Kaiser (2009), CFD simulations are used as a "numerical laboratory" to investigate the performance of solar chimneys under certain conditions, varying geometric and/or operating parameters.

In this work, different ways of modeling the air flow through a solar chimney are evaluated from numerical simulations with CFD techniques, using the OpenFOAM software. The simulations are performed in version 8 of the OpenFOAM variant which is published by the OpenFOAM Foundation (openfoam.org). The chimney from the work of Chen *et al.* (2003) is simulated, in which the authors built a laboratory model of a solar chimney with uniform heat flux on one of its walls, achieved through electrical heating. It is a vertical chimney (without inlet or outlet channels) suspended in still air at a uniform temperature, with height $H = 1.5$ m and variable wall-to-wall spacing. The case simulated in this work is one with 20 cm of wall-to-wall spacing and 400 $\frac{\mathrm{W}}{\mathrm{m}^2}$ imposed on the heated wall, in which Chen *et al.* (2003) measured a $0.024\ \frac{\mathrm{m}^3}{\mathrm{s}}$ volumetric airflow. Considering that the width of the tested chimney is 0.62 m, the volumetric airflow rate per unit of width of this case results in $0.0387\ \frac{\mathrm{m}^3/\mathrm{s}}{\mathrm{m}}$. Assuming that the ambient air in the tests is close to 20°C (value not reported by the authors) and then considering a density of approximately $1.16\ \frac{\mathrm{kg}}{\mathrm{m}^3}$ (because air is slightly heated in the chimney), this corresponds to a mass flow rate of about $0.045\ \frac{\mathrm{kg/s}}{\mathrm{m}}$. The basic outputs of the simulations are the velocity and temperature fields of the air inside the chimney, from which the mass air flow rate achieved is obtained, being this the main output variable of the performed simulations for this work.

2. METHODOLOGY

The `buoyantPimpleFoam` solver is used to perform the simulations in this work. This is a transient solver for buoyant flows of compressible fluids, for ventilation and heat transfer applications.

Although the width of the channel of the experimental solar chimney of the work of Chen *et al.* (2003) is not very large (in comparison to the height of the chimney or the wall-to-wall spacing), just the two-dimensional problem is considered. This is how simulations are usually carried out in the scientific papers about solar chimneys consulted for this work.

The chimney alone is taken as computational domain and the mesh taken into account is refined near the solid walls.

Only laminar simulations are performed, so no turbulence model is activated, because in the considered case the Rayleigh number, Ra, amounts to 8.11×10^{12}. This value is close to 10^{13}, around which the transition to turbulence occurs for the case of a solitary vertical plate that imposes a uniform heat flux to the fluid at rest, when the Prandtl numbers, Pr, are in the range that includes those of air and water, according to Bejan (2013). Chen *et al.* (2003) claim that transition to turbulence in the solitary vertical plate occurs in the range $2 \times 10^{13} < Ra < 10^{14}$, but that it is possible that in their experimental chimney it occurs for slightly lower values, due to the disturbances that occur at the inlet.

2.1 Equations of motion

The governing equations for air flows inside solar chimneys are the momentum equation, the continuity equation and the energy equation.

The momentum equation that solves the `buoyantPimpleFoam` is shown in Eq. (1):

$$\frac{\partial}{\partial t}(\rho \mathbf{v}) + \mathbf{div}(\rho \mathbf{v} \otimes \mathbf{v}) = gz\nabla\rho - \nabla p\_\mathrm{rgh} + \mathbf{div}(2\mu\mathbb{D}) \tag{1}$$

where $\frac{\partial}{\partial t}$ is the local derivative, ρ is the density, $\mathbf{v}$ is the velocity, $\mathbf{div}()$ is the divergence of a tensor field, $\otimes$ denotes the tensor product between two vectors, g is the magnitude of the gravitational field, z is a coordinate pointing in the opposite direction to the gravitational field vector, $\nabla()$ is the gradient of a scalar field, $p\_\mathrm{rgh} = p + \rho g z$ (with p being the pressure), μ is the dynamic viscosity, and $\mathbb{D}$ is the strain rate tensor. Notice that the terms $gz\nabla\rho - \nabla p\_\mathrm{rgh}$ are equivalent to $\rho\mathbf{g} - \nabla p$, where $\mathbf{g}$ is the gravitational field vector.

The continuity equation used in the `buoyantPimpleFoam` solver is shown in Eq. (2):

$$\frac{\partial \rho}{\partial t} + \mathrm{div}(\rho \mathbf{v}) = 0 \tag{2}$$

where $\mathrm{div}()$ is the divergence of a vector field.

The energy equation that is solved in the `buoyantPimpleFoam` is shown in Eq. (3):

$$\frac{\partial}{\partial t}(\rho e) + \mathrm{div}(\rho e \mathbf{v}) = \rho \mathbf{g} \cdot \mathbf{v} + \mathrm{div}(-p\mathbf{v}) - \mathrm{div}(\mathbf{q}) \tag{3}$$

where e is the total specific energy ($e = \frac{v^2}{2} + u$, being u the specific internal energy), $\cdot$ indicates the scalar product between two vectors and $\mathbf{q}$ is the heat conduction vector or heat flux.

Constant transport properties and specific heat are taken into account. To calculate the density, ρ, as a function of temperature, T, the OpenFOAM equation of state `Boussinesq` is considered. It contemplates variations of density in the same manner that is considered in the gravitational term under the Boussinesq approximation: $\rho = \rho_0 - \rho_0\beta_0(T - T_0)$, where ρ_0 is the density at a reference temperature, T_0, which is taken equal to that of the air entering the chimney (outside air, considered to be at 20ºC) and β_0 is the thermal expansion coefficient at T_0, that in the present work it is calculated using the ideal gas law. The remaining numerical values of the thermophysical properties used are taken from the air at atmospheric pressure table of Bergman and Lavine (2017).

Note that the Boussinesq approximation is not used. Even though ρ is calculated in the same way as in the gravitational term under the Boussinesq approximation, this solver takes density variations in all terms where it is present. According to Kundu and Cohen (2004), the Boussinesq approximation can be applied if the Mach number is low ($Ma < 0.3$, which implies velocities lower than 100 m/s for the case of air at normal pressure and temperatures), if sound or shock wave propagation is not considered, if the vertical scale of the flow is not very large ($H << c^2/g$, where c is the speed of sound, which implies chimney heights much lower than 10 km), and if the temperature differences in the fluid are small ($\Delta T\beta_0 << 1$, which for air in solar chimneys implies temperature differences much lower than 300°C). The first three conditions mentioned above are met for the study of the air flow in a solar chimney, but the last one is questionable because temperature differences of around tens of degrees are expected between the absorber wall and the air entering the chimney. Ferziger *et al.* (2020) warn that the use of the Boussinesq approximation with very large temperature differences (greater than 15°C for air) can lead to significant errors, and even solutions that are qualitatively wrong. However, all the works surveyed that involve CFD simulations in solar chimneys use the Boussinesq approximation for the equations to be solved.

2.2 Boundary conditions

For velocity, the no-slip condition is used on solid walls (absorber plate and transparent cover). Regarding temperature, it is imposed that air receives a constant and uniform heat flux from the absorber plate, with a value $q_\mathrm{w} = 400\frac{\mathrm{W}}{\mathrm{m}^2}$, and in the transparent cover two variants are considered: in one, heat flux that air receives from it is admitted to be zero and in another, a certain contribution of heat from this surface is considered, based on setting a constant and uniform temperature value there, $T_\mathrm{g} = 30$ºC (10ºC above the inlet air), which is representative of what Chen *et al.* (2003) measured on that surface when they imposed 400 $\frac{\mathrm{W}}{\mathrm{m}^2}$ using 20 cm of wall-to-wall spacing.

For the inlet and outlet sections, the temperature of incoming air is fixed equal to T_0 and for exiting flow the normal gradient of T is set to zero. Regarding velocity, for incoming flow it is imposed zero tangential component and for exiting flow it is considered zero normal gradient.

Before describing the boundary conditions imposed on the pressure, it is worth making some clarifications regarding the chimney that is sought to emulate, from the work of Chen *et al.* (2003). This is a vertical chimney (without inlet or outlet channels) suspended in still air that is at a uniform temperature. Since there are only pressure differences due to

hydrostatics between the air below the chimney and the air above it, the flow generated in the chimney is linked only to the stack pressure that occurs in it from the heating of the air inside it. That is, there is no external forcing, as would occur if the chimney took air from a different room than the one where it discharges and these were at different pressures.

Considering that the still air that would surround the chimney at the height of the inlet section is at a pressure p_0, then the boundary condition imposed there for the incoming flow is $p = p_0 - \rho_0 \frac{v^2}{2}$. Since the still air that would surround the chimney at the height of the exit section is, by hydrostatics, at $p_0 - \rho_0 g H$, then the boundary condition imposed there for the exiting flow is $p = p_0 - \rho_0 g H$, which sets a uniform value to the pressure at this horizontal boundary. For incoming flows through the outlet section (counterflows), $p = p_0 - \rho_0 g H - \rho_0 \frac{v^2}{2}$ is imposed.

Figure 3 (left) resumes the boundary conditions applied for each of the boundary surfaces of the solar chimney considered for the simulations.

2.3 Implementation of pressure boundary conditions in OpenFOAM

The OpenFOAM distribution includes the boundary condition `totalPressure`, which if applied to the pressure would do exactly what is intended in this case, because this boundary condition imposes a fixed value (previously set) to the pressure for exiting flows, and imposes that same value minus the kinetic term for incoming flows. Since `buoyantPimpleFoam` uses p_rgh instead of pressure p in the momentum equation, the boundary conditions in this OpenFOAM solver are imposed on p_rgh.

To apply the `totalPressure` boundary condition to the p_rgh field, certain care must be taken, because what ends up being imposed on the pressure p (and therefore the physical meaning of what ends up being imposed) depends on where the origin of the vertical coordinate, z, is located in the computational domain.

In this case, if the origin of the vertical coordinate is set at the height of the chimney inlet section, it is not possible to impose what is intended on the pressures with this boundary condition that OpenFOAM includes. For example, if the same value of p_rgh is set in the inlet and outlet sections, which is what would be done if working with $p_{\mathrm{mov}} = p + \rho_0 g z$ (as is done when using the Boussinesq approximation) instead of with $p\_\mathrm{rgh} = p + \rho g z$, in the simulations with the origin of the vertical coordinate in the inlet section the air cannot exit the chimney freely. Although the air is heated against the absorber wall and rises close to it, when it approaches the outlet section at the top of the chimney it seems as if it hits a "cover" that does not let it out and ends up flowing towards the other wall, going down when it hits the cover plate, to end up forming a series of vortices of air trapped in the chamber. Figure 3 (right) shows velocity magnitude fields at instants close to the beginning of a simulation, where the behaviour described in the previous sentence can be observed.

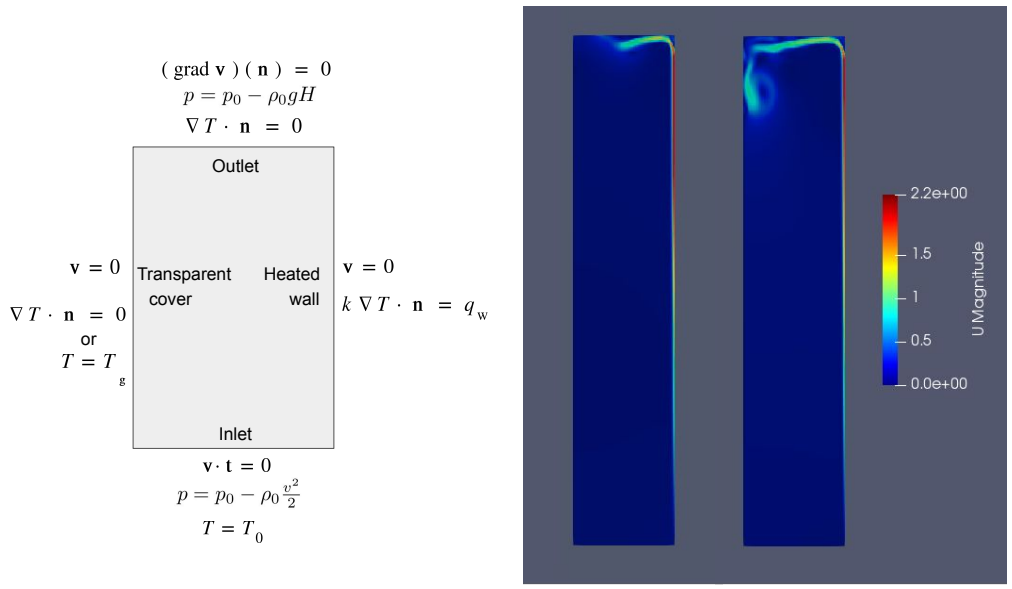

Figure 3: Boundary conditions applied in the simulations (left) and magnitude of the velocity at two instants at the beginning of a simulation carried out with the origin of the vertical coordinate at the entrance of the chimney (right).

This has to do with the fact that in this case, the exiting flows through the top of the chimney are actually subjected to a pressure $(\rho_0 - \rho) g H$ greater than what is intended. This amount is of the order of magnitude of the stack pressure achieved in the chimney, which explains why the air cannot escape when it reaches the top, because there it encounters a downward force similar in magnitude to the one that generates the upward movement.

With the boundary condition `totalPressure` it is not possible to impose $p\_\mathrm{rgh} = p_0 - (\rho_0 - \rho) g H$, which is what p_rgh needs to fulfill for the pressure to equal $p = p_0$, because the value to be imposed depends on the density of the air leaving the domain, which is not previously known (it is a result of the simulation). If the origin of the vertical coordinate

was somewhere else, what would have to be imposed is $p\_\mathrm{rgh} = p_0 - (\rho_0 - \rho)gh$, where h is the z coordinate evaluated in the chimney outlet section. So if the origin of the vertical coordinate was located at the height of the output section, so that $h = 0$ is set, imposing $p\_\mathrm{rgh} = p_0$ is equivalent to setting $p = p_0$.

For air flows entering the domain, whether in the inlet or outlet section (from a counterflow), the position of the z origin has no consequences on the pressure boundary conditions for the chimney problem being simulated. This has to do with the fact that air always enters at the reference temperature, T_0, due to the boundary condition imposed on the temperature, which causes the density of the entering air to be the reference density, ρ_0. Therefore, the pressure differences of the type $(\rho_0 - \rho)gh$ that occur for the exiting flows end up being null for the incoming flows.

According to the reasoning presented, if in this solar chimney case the origin of the vertical coordinate is placed at the height of the outlet section of the chimney, then setting the same value of p_rgh in the boundary condition `totalPressure` at the inlet and outlet effectively imposes what is intended on the pressure. In the simulations that consider this, results that behave as expected in the output section are achieved, as can be seen in Fig. (5) and in Fig. (6).

2.4 Comparison of results for different thermal boundary conditions on the transparent cover

Before discussing the results obtained, it is worth mentioning that prior to carrying out the simulations for which the results are presented below, a satisfactory validation of the chimney case that was prepared in OpenFOAM was carried out, by comparing against results of numerical simulations performed by Khanal and Lei (2014). The simulations carried out for this work with OpenFOAM gave very similar results to those presented by Khanal and Lei (2014) for one of their simulations, for which they show the evolution of the mass flow rate as a function of time and the steady-state velocity profile at the chimney exit. The steady-state mass flow value was almost identical (96 is the dimensionless value obtained from the figure the presented, and 97 is the correspondent value from the validation of the chimney case for this work) and the steady-state velocity profile was very similar, as Fig. (4) shows. These simulations would not have to give exactly the same results, because Khanal and Lei (2014) considered the Boussinesq approximation in the equations of motion and the `buoyantPimpleFoam` solver takes density variations in all terms where it is present.

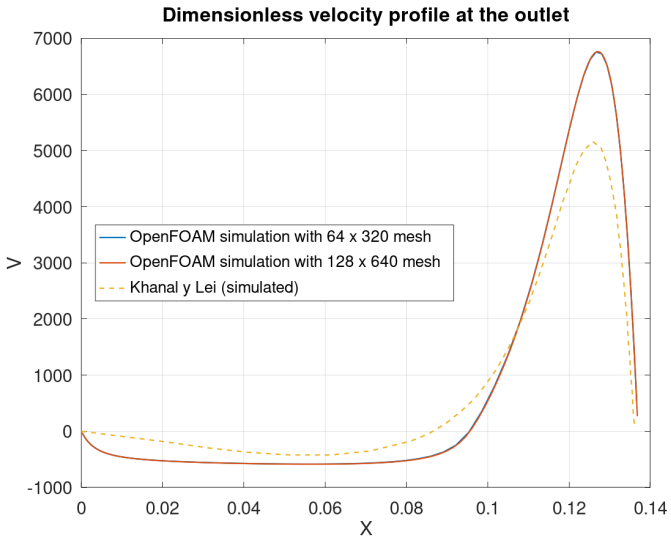

Figure 4: Dimensionless velocity profile at the outlet section, obtained in OpenFOAM simulations validation with Khanal and Lei (2014) simulation results. Profiles obtained with two different mesh densities are presented, to show that with these mesh densities results are not mesh dependent.

As mentioned, simulations are performed for two different boundary conditions on the transparent cover, one in which the heat transferred by this surface to the air is assumed to be zero, and another in which a contribution of heat to the air is contemplated by imposing a constant and uniform temperature value (30ºC), representative of what was measured by Chen *et al.* (2003) on that surface when they imposed 400 $\frac{\mathrm{W}}{\mathrm{m}^2}$ using a 20 cm wall-to-wall spacing.

Results obtained for the adiabatic boundary condition on the transparent cover can be seen in Fig. (5).

The simulations shown in this work were performed in a 64 x 320 mesh (horizontal x vertical). Results with a 128 x 640 mesh were almost identical.

The velocity field figure shows a very thin boundary layer near the absorber wall, with very low velocities at the bottom of the chimney. Its thickness increases with height, as well as the velocity modules. Velocities inside the boundary layer are essentially vertical, in the upward direction.

The boundary layer that is formed is very similar to that which occurs in a solitary vertical plate that provides uniform heating to the fluid at rest in which it is immersed. The main difference between this flow and the one in the simulated

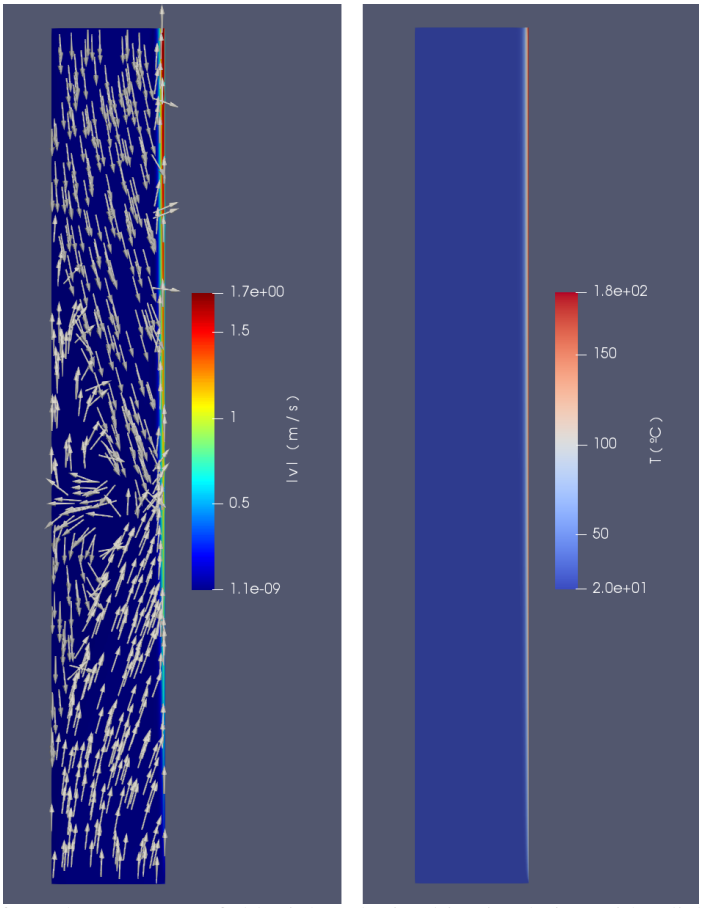

Figure 5: Velocity field (left) and temperature field (right) obtained in simulation with adiabatic boundary condition in transparent cover. Arrows indicate direction of vector **v**, but not its magnitude, which is indicated by the color scale.

chimney is how the boundary layer is fed with the distant fluid. In the solitary plate case the fluid arrives "from infinity" in a purely horizontal direction. But in the chimney case there is another wall (the transparent cover) very close to the heated one, so air cannot arrive to the latter in the same manner. In the lower area of the chimney, up to approximately half the height, the boundary layer is supplied with air entering through the inlet section. This air enters with vertical direction at very low speeds, and as it goes up its velocity gets slightly inclined towards the absorbing wall, until it reaches the boundary layer, where an abrupt acceleration takes part. After a certain height, the air supply for the boundary layer begins to arrive from the outlet section of the chimney, from a counterflow that establishes there between the transparent cover and the boundary layer at that height. The air that enters vertically with very low magnitude downward velocities, gradually changes its velocity direction towards the absorber plate, until it suddenly turns around and is finally dragged by the ascending current within the boundary layer.

Qualitatively, the velocity field obtained in this simulation is different from that of the experiments of Chen *et al.* (2003), because in their experiments a counterflow was not observed at the exit of the chimney. There are also quantitative differences, because the mass flow rate of the simulation, $8,0 \times 10^{-3}\ \frac{\mathrm{kg/s}}{\mathrm{m}}$, is approximately 5 times smaller than that derived from the results of Chen *et al.* (2003), $4,5 \times 10^{-2}\ \frac{\mathrm{kg/s}}{\mathrm{m}}$.

Simulation results are closer to experimental ones when heat from the transparent cover is taken into account, since in experiments there is some radiative heat from the surface that acts as absorber plate to the surface that acts as transparent cover, from which air also heats up near that surface. Results obtained when taking into account the temperature boundary condition imposed on the transparent cover to contemplate heat transfer to air are shown in Fig. (6).

The velocity field is quite different from that of the case with an adiabatic cover plate, since in this instance there is no counterflow (velocities are essentially upward, all along the chimney), in addition to having velocities near the cover plate well above the velocity values near the mid-plane between both walls. Regarding the temperature field, the figure shows how air near the cover plate now slightly heats, in addition to the heating near the absorber wall, already present in the previous simulation.

The mass flow rate achieved in the simulation that considers air heating from the cover plate, $2,6 \times 10^{-2}\ \frac{\mathrm{kg/s}}{\mathrm{m}}$, is much closer to that derived from the results of Chen *et al.* (2003), although it is still smaller (simulation value is approximately 60% of experimental value).

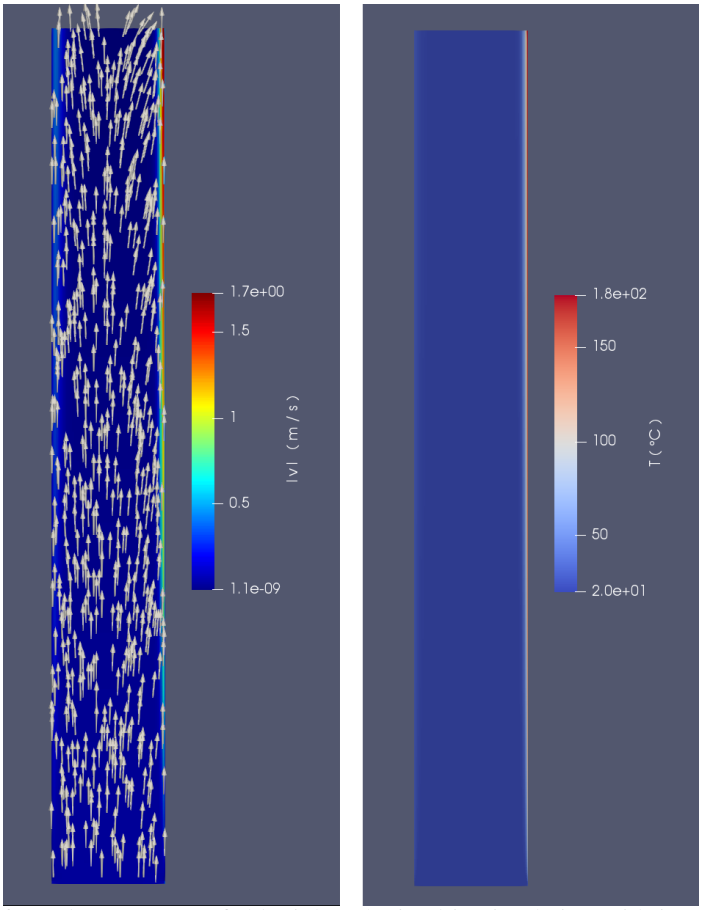

Figure 6: Velocity field (left) and temperature field (right) obtained in simulation with imposed temperature boundary condition in transparent cover. Arrows indicate direction of vector **v**, but not its magnitude, which is indicated by the color scale.

Figure (7) complements the results shown for the case with imposed temperature boundary condition in the transparent cover. It shows the velocity profile obtained in the simulations at a height 1,10 m above the inlet section, which is quite close to the outlet section (chimney height is 1,5 m). The experimental results measured by Chen *et al.* (2003) at the mentioned height for this case are superimposed.

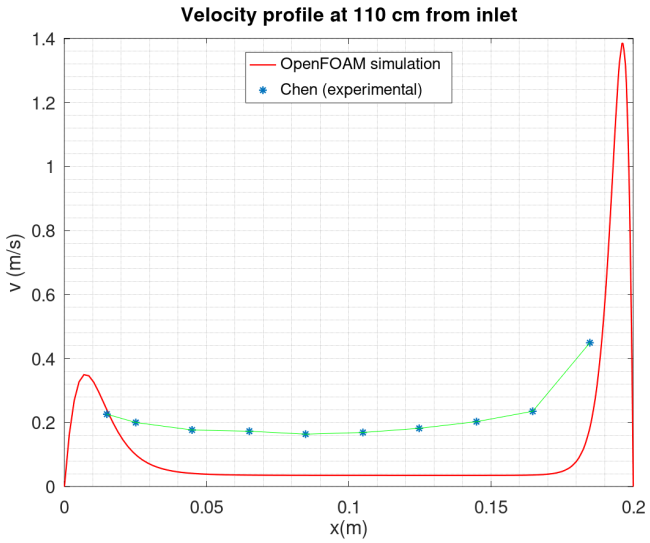

Figure 7: Velocity profile 1,10 m away from the inlet section, obtained in OpenFOAM simulation with imposed temperature boundary condition in transparent cover.

It can be seen that values of the velocity near the cover plate, even though they are much smaller than those near the absorber plate, are much larger than those near the mid-plane between both walls.

It is worth mentioning that 16 of the 64 cells in the horizontal direction are contained in the boundary layer formed near the absorber wall at the outlet section (in the 17th cell of the outlet section the value of the vertical velocity drops below 1% of the maximum achieved at that height).

3. CONCLUSIONS

In OpenFOAM 8 solver `buoyantPimpleFoam`, which works with $p\_\mathrm{rgh} = p + \rho g z$ instead of pressure (or motion pressure, $p_{\mathrm{mov}} = p + \rho_0 g z$), imposing uniform pressure on exiting flows with the `totalPressure` boundary condition requires that the origin of the vertical coordinate be at the height of the outlet section of the chimney. If the origin of z is located at the height of the inlet section, when the same value of p_rgh is set at the outlet as at the inlet, air does not flow freely outwards when arriving at the outlet section, because pressures imposed are $(\rho_0 - \rho) g H$ greater than what makes physical sense, and that amount is of the same order of magnitude as the stack pressure generated in the chimney, which gives rise to the upward movement of the air inside it. This aspect of the `buoyantPimpleFoam` makes solving buoyant convective flows in open domains quite tricky.

Modeling the chimney assuming that air receives negligible heat from the cover plate does not provide results matching experimental measurements. There are important differences both quantitatively, since the mass flow achieved in simulations is much smaller than that measured experimentally, and qualitatively, because in simulations there is a counterflow that is not present in experiments. The fact that heat provided by the cover plate (which heats up due to radiation exchange with the absorber wall) is somehow taken into account substantially improves the aspects mentioned, since the steady-state mass flow obtained in the simulations is much closer to that of the experimental measurements (same order of magnitude, although still lower) and the counterflow no longer occurs when reaching the steady state. Incorporation of a turbulence model is considered as future work since, even in the simulations that include heating from the cover plate, differences that could be linked to diffusive effects of a possible presence of turbulent phenomena in the experimental chimney are observed. Three-dimensional simulations are also considered as future work, since some of the differences could be explained by some phenomena that two-dimensional simulations are not capable of taking into account.

4. ACKNOWLEDGEMENTS

This work was part of the thesis carried out by Daniel Croza in the Master's program in Mechanical Engineering at the Universidad de la República (UdelaR) in Uruguay, for which he received a scholarship from the Comisión Académica de Posgrado (CAP) of the UdelaR.

5. REFERENCES

Bansal, N.K., Matur, R. and Bhandari, M.S., 1993. "Solar chimney for enhanced stack ventilation". *Building and Environment*, Vol. 28, No. 3, pp. 373–377.

Bejan, A., 2013. *Convection Heat Transfer*. John Wiley & Sons, 4th edition.

Bergman, T.L. and Lavine, A.S., 2017. *Fundamentals of Heat and Mass Transfer*. John Wiley & Sons, 8th edition.

Chen, Z.D., Bandopadhayay, P., Halldorsson, J., Byrjalsen, C., Heiselberg, P. and Li, Y., 2003. "An experimental investigation of a solar chimney model with uniform wall heat flux". *Building and Environment*, Vol. 38, No. 7, pp. 893–906.

Ferziger, J.H., Perić, M. and Street, R.L., 2020. *Computational Methods for Fluid Dynamics*. Springer International Publishing, 4th edition.

Khanal, R. and Lei, C., 2014. "A scaling investigation of the laminar convective flow in a solar chimney for natural ventilation". *International Journal of Heat and Fluid Flow*, Vol. 45, pp. 98 – 108.

Kosut, J., 2017. *Chimenea solar con acumulación de calor para acondicionamiento térmico pasivo de edificios*. Master's thesis, Universidade Federal do Rio Grande do Sul.

Kundu, P.K. and Cohen, I.M., 2004. *Fluid Mechanics*. Elsevier Academic Press, 3rd edition.

Miyazaki, T., Akisawa, A. and Kashiwagi, T., 2006. "The effects of solar chimneys on thermal load mitigation of office buildings under the japanese climate". *Renewable Energy*, Vol. 31, pp. 987 – 1010.

Zamora, B. and Kaiser, A., 2009. "Optimum wall-to-wall spacing in solar chimney shaped channels in natural convection by numerical investigation". *Applied Thermal Engineering*, Vol. 29, pp. 762 – 769.

6. RESPONSIBILITY NOTICE

The authors are solely responsible for the printed material included in this paper.